

# Thermodynamic study of a membraneless electrochemical process for the hydrogen and oxygen high-pressure generation

Andrii Shevchenko  
Hydrogen Energetics  
Department

A.M. Pidhorny Institute of  
Mechanical Engineering  
Problems of NASU,  
Kharkiv, Ukraine

[shevchenkoandrii84@gmail.com](mailto:shevchenkoandrii84@gmail.com)

ORCID: 0000-0002-6009-2387

Nguyen Tien Khiem  
Vietnam Academy of Science and  
Technology,

Hanoi, Viet Nam

[ntkhiem@imech.vast.vn](mailto:ntkhiem@imech.vast.vn)

ORCID: 0000-0001-5195-2704

Bui Dinh Tri  
Vietnam Academy of Science and  
Technology,

Hanoi, Viet Nam

[bdtri@vast.vn](mailto:bdtri@vast.vn)

Anatolii Kotenko  
Hydrogen Energetics  
Department

A.M. Pidhorny Institute of  
Mechanical Engineering  
Problems of NASU,  
Kharkiv, Ukraine

[kotenko19580820@gmail.com](mailto:kotenko19580820@gmail.com)

ORCID: 0000-0003-2715-634X

## Abstract

The article presents the results of the thermodynamic analysis of the electrochemical process of hydrogen and oxygen high-pressure generation. This process can improve the energy efficiency of the membraneless electrolysis method.

The method is based on the use of a gas-absorbing electrode with a highly developed contact surface of the electrode material with the electrolyte. The electrochemical activity of the gas-absorbing electrode material (Fe(g)) is higher in its characteristics than that of platinum-coated electrodes and exceeds them in the efficiency of the electrolysis process. The electricity consumption required for the production of hydrogen and oxygen is in the range of 3.95 kWh/m<sup>3</sup> to 4.16 kWh/m<sup>3</sup>. It should also be noted that this process is cyclic, consisting of a half-cycle of hydrogen evolution and a half-cycle of oxygen evolution. The distribution of the energy consumption by half-cycles is 0.88 kWh/m<sup>3</sup> per H<sub>2</sub> ↑; 3.28 kWh/m<sup>3</sup> on O<sub>2</sub> ↑ respectively. The material of the gas-absorbing electrode (Fe (g)) chemically binds the oxygen when it acts as the anode, while the hydrogen is evolved at the cathode (Ni). The reverse of the polarity allows the hydrogen to be chemically bound by the cathode material (Fe (g)) and the oxygen gas to be evolved at the anode (Ni). The cyclic operation of the electrochemical cell makes it possible to stop the usage of proton-exchange membranes, which results in a significant increase in the operating pressure of the generated gases (up to P = 20.0 MPa). This pressure is achieved not because of the use of compressor equipment, but due to the isochoric process of electrochemical production of high-pressure hydrogen and oxygen. The above advantages contribute to the successful implementation of an innovative electrolyzer as an element of a buffer storage system for a secondary energy carrier (hydrogen) in energy technology complexes using alternative energy sources.

**Keywords:** electrolyzer, anode, cathode, hydrogen, oxygen, high-pressure, alternative energy sources.

## I. INTRODUCTION

Hydrogen (H<sub>2</sub>) is a gas with a very low density of 0.0813 g/l under normal conditions (at 248 K and 0.1 MPa) [1] and therefore there are many difficulties in the development of efficient and compact

storage of H<sub>2</sub>. The low efficiency of mechanical compressors for hydrogen (15-45%) and oxygen (13-17%) leads to an additional increase (by 10-15%) in the unit cost of electricity for the production and storage of gases [2]. When the hydrogen is compressed to P = 70.0 MPa, its bulk density of the stored energy is ρV(H<sub>2</sub>) = 5.6 MJ/L (40 g H<sub>2</sub>/L) [3]. Therefore, the development of electrochemical technologies for generating hydrogen under high operating pressure and minimal power consumption is promising and relevant for hydrogen power engineering [4].

Distinctive features of water electrolysis from the other methods of hydrogen production are: simplicity of the technological scheme, availability of water as a feedstock, easiness of maintenance of the electrolysis installations, high reliability of the operation. All these make it possible to successfully combine the given method with the usage of other renewable energy sources (sun, wind, etc.) [5, 6]. The main disadvantage of the electrochemical method for producing hydrogen is its high energy consumption.

The authors of the article have developed and successfully tested the technology for the production of high-pressure hydrogen both in laboratory and field conditions [7, 8]. The main difference of the technology compared to the traditional electrolysis technologies is the usage of variable valence metals as materials of electrodes [9].

The technological and design features of this electrolysis technology make it possible to successfully use it as a buffer energy storage in an energy-technological complex using alternative energy sources [10].

## II. PURPOSE AND OBJECTIVES OF THE STUDY

The main goal of the study is to determine the regularities of the redox reactions of the cyclic process of the gas-absorbing electrode. The process understanding makes it possible to secure the membraneless production of high-pressure hydrogen and oxygen. The determination of the electric potential of chemical reactions and the overvoltage of gas evolution at the cathode and anode allows composing the energy balance of a membrane-less electrolysis process. Thermodynamic analysis reveals the main distinguishing features of the standard and the proposed electrolysis system. Based on the results of the analysis, it is possible to develop a set of methods for reducing irreversible losses and increasing the energy efficiency of the cyclic method for

the electrochemical production of high-pressure hydrogen and oxygen.

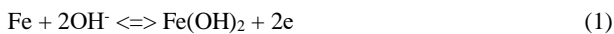
Optimization of the electrochemical system operation modes, the development of design and technological solutions aimed to reduce the energy consumption of the hydrogen and oxygen production process without the use of compression devices can be implemented as follows:

- selection and optimization of the structure of electrode materials;
- selection of electrode material with low gas evolution potential;
- optimization of the algorithm of operation and temperature conditions;
- optimization of the design of the main elements of the electrolysis system.

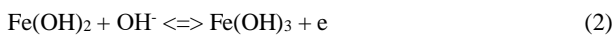
### III. ELECTROCHEMICAL PROCESSES ON THE ELECTRODE ASSEMBLY USING A GAS-ABSORBING ELECTRODE

The authors of the article have developed an innovative membraneless electrochemical method for the decomposition of a liquid alkaline electrolyte. The method is based on the use of a gas-absorbing substance with a highly developed contact surface of the electrode material with the electrolyte.

The use of sponge iron as the oxygen-bonding electrode material is consistent with the reaction:



With the prolonged operation of the active mass of the electrode, deeper oxidation of Fe occurs:



The electrochemical production of hydrogen and oxygen on the half-cycle of H<sub>2</sub> evolution corresponds to the transition of Fe (II) to Fe (III), and the half-cycle of O<sub>2</sub> evolution corresponds to the electrochemical reduction of Fe (Fig. 1).

The material of the gas-absorbing electrode (Fe (g)), in a state of the anode, chemically binds oxygen, while hydrogen is freely released on the other electrode, the cathode (Fig. 1 a). The reverse of the polarity allows the hydrogen to be bound at the cathode (Fe (g)) and the oxygen to be released at the anode (Fig. 1 b).

Fe(OH)<sub>2</sub> retains a spongy structure and has an expansive contact surface with the electrolyte. Polarization during the oxidation of the electrode active mass is caused by a slowdown in the diffusion of OH<sup>-</sup> ions. The diffusion rate decreases with an increase in the thickness of the reacted Fe-layer.

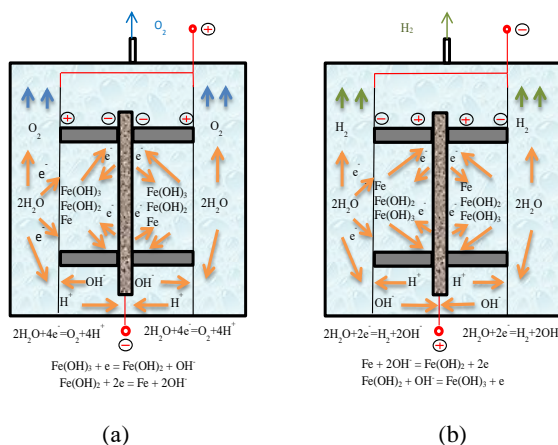


Figure 1. Diagrams of electrochemical processes occurring on electrode assemblies with a gas-absorbing electrode: a - half-cycle of oxygen evolution; b - half-cycle of hydrogen evolution.

The evolution of gaseous hydrogen occurs at the passive electrode (cathode) (Fig. 1 a). It is advisable to use Fe or Ni as a passive electrode. The overvoltage of hydrogen evolution on Ni is 210 mV, and on Fe is 80 mV (see Table 1).

Table 1. Overvoltage of hydrogen and oxygen evolution [11]

Electrode material	Overvoltage, mV	
	H <sub>2</sub>	O <sub>2</sub>
Pt (platinized)	0	250
Fe	80	250
Pt (smooth)	90	450
Ni	210	60

The low overvoltage of hydrogen and oxygen evolution at the passive Ni-electrode allows obtaining these gases directly from the very beginning of the electrochemical decomposition of the water (current density from 200 A/m<sup>2</sup> to 600 A/m<sup>2</sup>).

### IV. ANALYSIS OF THERMODYNAMIC PROCESSES OF LIQUID ELECTROLYTE DECOMPOSITION IN ELECTROCHEMICAL SYSTEMS FOR PRODUCING HYDROGEN AND OXYGEN

The energy assessment is based on the description of a unified hydrogen production model. It consists of stationary balances of energy, entropy and mass, as well as the ideal gas equation. Based on this, reversible energy demand is used to identify internal thermodynamic losses. Additional consideration of the irreversibility allows determining the loss of efficiency, taking into account the specific characteristics of the device.

The basis for the energy balance of a standard electrolysis system is the irreversible energy loss when current passes through the electrolyte Fig. 2 [12].

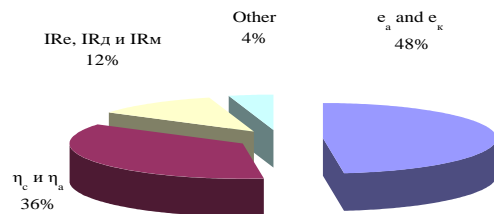


Figure 2. Voltage Distribution on Electrodes in the Electro-Chemical Cell.

The energy balance of the electrolysis system can be written as an equation:

$$E = e_a + e_c + \eta_c + \eta_a + e_{cp} + e_d + IR_e + IR_m + IR_c \quad (3)$$

where: e<sub>a</sub> and e<sub>c</sub> – reversible thermodynamic potentials of anode and cathode; η<sub>c</sub> и η<sub>a</sub> – overvoltage of the release of hydrogen on the cathode and oxygen on the anode; e<sub>cp</sub> и e<sub>d</sub> – concentration and diffusion polarizations; I – current; R<sub>e</sub>, R<sub>m</sub> и R<sub>c</sub> – resistance of the electrolyte, metal conductors and contacts in the cell.

The thermodynamically reversible potentials of the anode and cathode are determined from the formula:

$$e_{a(c)} = \Delta H_{298}^{0(\text{reaction})} / nF \quad (4)$$

where: ΔH<sup>0</sup><sub>298(reaction)</sub> – enthalpy of reaction J·mol<sup>-1</sup>; n – the amount of a substance involved in the reaction; F – Faraday number 96570 A·s.

The free energy and the enthalpy are calculated for conditions with temperatures of 298 K and pressure of 101.3 kPa. The enthalpy of reaction (1) at the active electrode is defined as:

$$\Delta H_{298}^0(1) = \Delta H^0 \text{Fe(OH)}_2 - 2\Delta H^0 \text{OH}^- \quad (5)$$

and is 104.315 kJ mol<sup>-1</sup>, and the enthalpy of the reaction (2) is determined as:

$$\Delta H_{298}^0(2) = \Delta H^0 \text{Fe(OH)}_3 - \Delta H^0 \text{Fe(OH)}_2 - \Delta H^0 \text{OH}^- \quad (6)$$

and is 36.267 kJ·mol<sup>-1</sup>.

Table 2 shows the calculated values of the free energy  $\Delta G^0$  and the enthalpy  $\Delta H^0$  of the reaction components at the gas-absorbing electrode.

**Table 2. Free energy and enthalpy of reactions**

The chemical compound	Free energy $\Delta G^0$ , J·mol <sup>-1</sup>	Enthalpy $\Delta H^0$ , J·mol <sup>-1</sup>
OH <sup>-</sup>	157360	228850
H <sub>2</sub> (gas)	0	0
O <sub>2</sub> (gas)	0	0
Fe(OH) <sub>2</sub>	480008	562015
Fe(OH) <sub>3</sub>	700050	827132

The voltage of the active mass oxidation reaction at the anode  $e_a$  is determined following equation (4) and for the reaction (1) is 0.54 V, and for the reaction (2) is 0.19 V.

The voltage  $E$  of the half-cycle of hydrogen evolution (see Fig. 2), considering the active mass oxidation reaction at the anode and the evolution of hydrogen at the cathode, is determined according to equation (3) and for the reaction (1) is 0.33 V, and for the reaction (2) it is 0.52 V.

The thermoneutral voltage is equal to the cell voltage in a hypothetical isobaric-isothermal process, in which there is no heat and mass exchange with the external environment and all the energy required for the reaction (the sum of the required heat and work) is supplied in the form of electricity.

The thermoneutral voltage  $E_q$  is practically constant. Considering the heat of evaporation, it is equal to  $E_q = 1.481$  V, and during the electrolysis of water vapor it is  $E_q = 1.25$  V [13].

The share of the work required for water decomposition in relation to the total energy consumption in the electrochemical process  $\eta$  is equal to the  $E_T / E_q$  ratio. Since  $E_T$  for water decreases with increasing temperature (at atmospheric pressure  $dE_T/dT = -0.25$  mV·K<sup>-1</sup>), then as the temperature rises, the share of the heat increases, and at  $T = 5000$  K. Practically all the energy required for water decomposition is used in the form of heat ( $\eta \approx 0$ ).

The dependences of  $E_T$  and other reaction parameters on the temperature are given in Table 3,

**Table 3. Theoretical values of EMF and energy consumption in the reaction of water decomposition (14.7 psi.)**

Reaction parameter	Temperature K							
	298	353	423	473	573	773	1273	2272
$E_T$ , V	1.23	1.18	1.15	1.10	1.04	0.95	0.80	0.50
$\eta$	0.83	0.80	0.92	0.88	0.83	0.76	0.64	0.40
$W_T^{\text{electric}}$ , kWh·m <sup>-3</sup>	2.94	2.82	2.75	2.63	2.49	2.27	1.91	1.20
$W_T^{\text{heat}}$ , kWh·m <sup>-3</sup>	0.60	0.72	0.24	0.36	0.5	0.72	1.08	1.79

where the theoretical values of  $W_T^{\text{electric}}$  are determined from the equation [14]:

$$W_T^{\text{electric}} = 2.394 E_T = 2.394 E_q \eta. \quad (7)$$

The theoretical values of  $W_T^{\text{heat}}$  are obtained from the formula [14]

$$W_T^{\text{heat}} = 2.394 (E_q - E_T) = 2.394 E_q (1 - \eta). \quad (8)$$

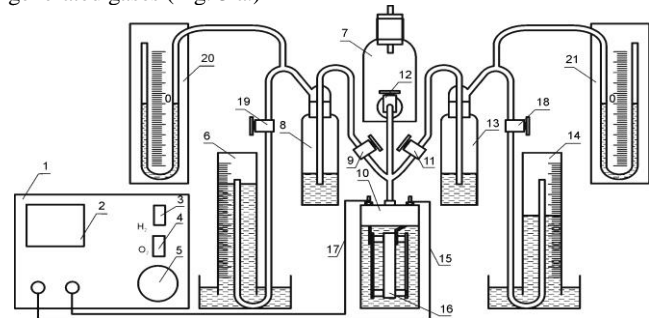
The decrease in the voltage value of the electrochemical decomposition of a liquid alkaline electrolyte (equation 3) in the proposed method for the hydrogen and oxygen generation was achieved due to:

- the exclusion of the voltage drop across the proton exchange membrane  $IR_m$ , due to its absence from the energy balance (equation 3);
- the reduction of the overvoltage values of the hydrogen evolution at the cathode and oxygen evolution at the anode  $\eta_k$  and  $\eta_a$ , since gas evolution occurs only at one of the electrodes.

## V. EXPERIMENTAL STUDY OF ELECTROCHEMICAL ACTIVITY AND CHARACTERISTICS OF ELECTRODE MATERIALS

A laboratory setup has been created in order to simulate the processes in an electrochemical cell for experimental studies of the electrochemical activity and electrochemical characteristics of electrode materials in cathode-anode systems.

Fig. 3 shows a functional diagram of the developed laboratory setup, which consists of: a reactor, main pipelines, separators, a tank with distilled water, a monitoring and control power supply unit, and a system for measuring the flow characteristics of the generated gases (Fig. 3 a.)



(a)



(b)

Figure 3. Functional diagram of a laboratory setup with an electrochemical cell: 1 - a monitoring and control power supply unit; 2 - digital indicator IC 412.3; 3 - power switch; 4 - hydrogen and oxygen half-cycle power switch; 5 - current control handle; 6 - oxygen measuring vessel; 7 - buffer tank H<sub>2</sub>O; 8 - oxygen separator; 9 - oxygen line valve; 10 - electrolysis cell; 11 - hydrogen line valve; 12 - valve for filling the hydraulic system with electrolyte; 13 - hydrogen separator; 14 - hydrogen measuring vessel; 15, 17 - electric wires; 16 - electrode assembly; 18, 19 - shut-off valves for hydrogen and oxygen lines; 20, 21 - U-shaped



differential pressure gauges for oxygen and hydrogen lines; a - laboratory setup diagram; b - photo of an electrochemical cell.

In the upper part of the reactor, there are power supply terminals, a fitting for an electrolyte inlet to the reaction zone and a gas outlet fitting, above which there is a three-way valve for dividing the gas-liquid channel into oxygen and hydrogen mains (Fig. 3 b). The electrode assembly is located in the internal section of the reactor; the reactor is filled with a 25% aqueous solution of KOH with the electrolyte density of 1.21 mg/l [15].

The diagram of the main elements and the design of the experimental sample of the electrode assembly are shown in Fig. 4.

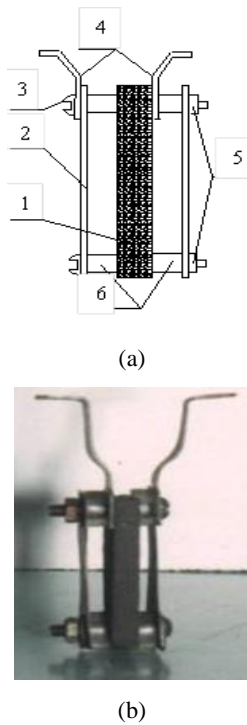


Figure 4. Schematic and experimental sample of the electrode assembly: 1- gas absorbing electrode (active); 2 - gas evolving electrode (passive); 3 - screws; 4 - current leads; 5 - screw-nut; 6 - spacer dielectric sleeves; a - electrode assembly diagram; b - experimental sample.

The three pairs of electrodes were defined for the experimental studies: 1 – Fe(g)-X18H15; 2 – Fe(g)-Fe; 3 – Fe(g)-Ni (Fig. 5).

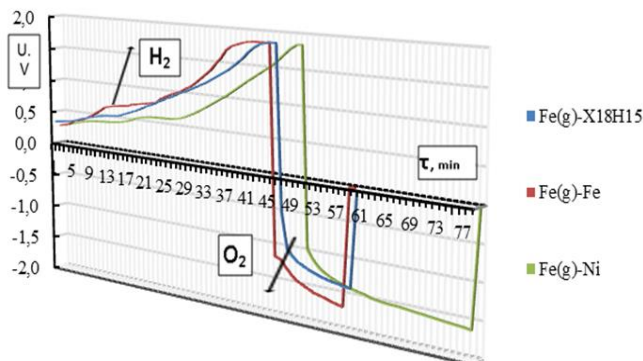


Figure 5. The sequence diagram of the change in the voltage of hydrogen and oxygen release during electrolysis with electrode combinations: 1. Fe(g)-X18H15; 2. Fe(g)-Fe; 3. Fe(g)-Ni.

A comprehensive experimental study was carried out in two stages.

The first stage of the experimental study was aimed to determine the voltage threshold value for the point when the gas began to evolve from two electrodes at the same time. On the half-cycle of the hydrogen evolution, this value was 1.8 V, and on the half-cycle of the oxygen evolution, it corresponded to 1.7 V (at the operating current density  $J = 0.02 \text{ A/cm}^2$ , or  $200.0 \text{ A/m}^2$ ), for the selected pairs of electrodes (Fe(g)-X18H15; Fe(g)-Fe; Fe(g)-Ni). Figure 6 shows the results of the first stage of the experimental study.

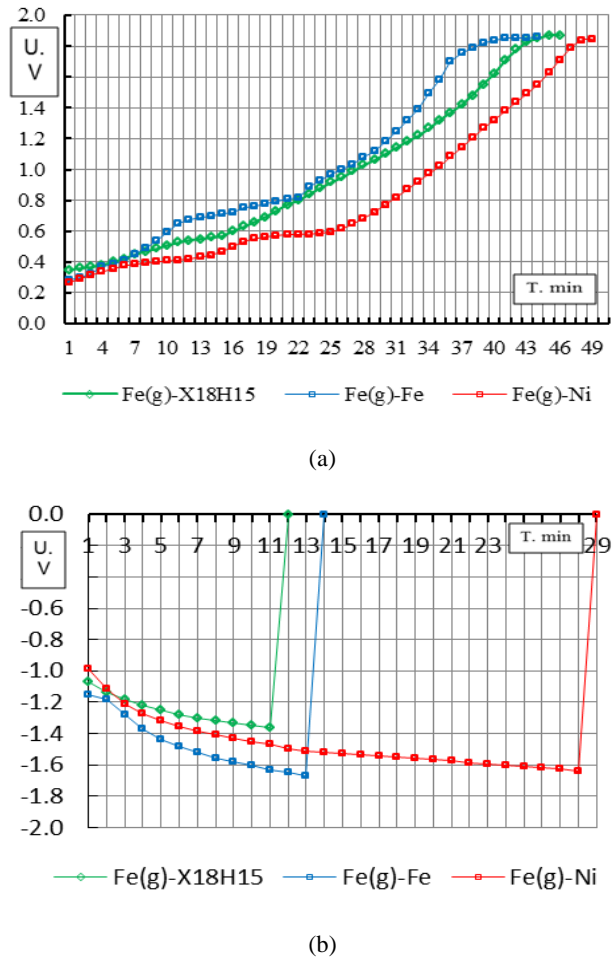
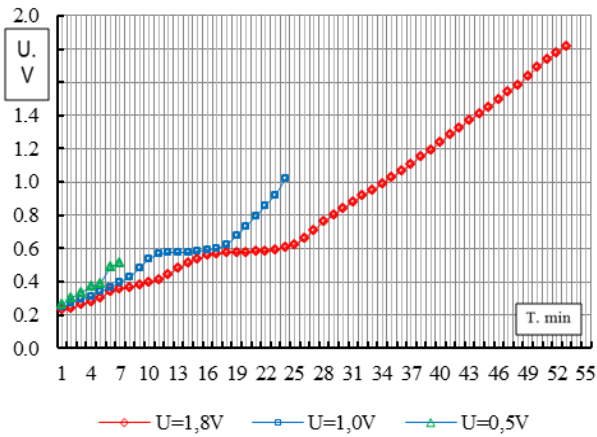


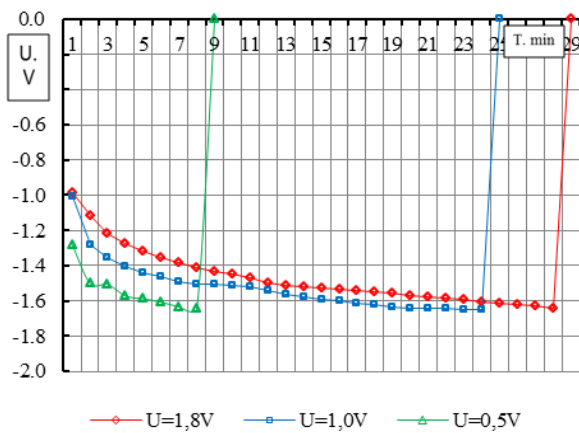
Figure 6. The sequence diagram of the voltage change of the membraneless high-pressure hydrogen generator, at  $J = 0.02 \text{ A/cm}^2$  with the electrode twins: 1. Fe(g)-X18H15; 2. Fe(g)-Fe; 3. Fe(g)-Ni: (a) - the half-cycle of  $\text{H}_2$  generation; (b) - the half-cycle of  $\text{O}_2$  generation.

The analysis of the study results has shown that on the hydrogen half-cycle (Fig. 6 a), the voltage of the onset of hydrogen evolution was 1.8 V and did not depend on the electrode materials (Fe(g)-X18H15; Fe(g)-Fe; Fe(g)-Ni), although it depended on the operating current density  $J = 0.02 \text{ A/cm}^2$ . On the half-cycle of oxygen evolution (Fig.6 b), the voltage of the onset of the oxygen evolution was 1.7 V, and the half-cycle time depended on both the electrode materials and the operating current density.

The second stage of the experimental study was aimed to prevent the simultaneous release of hydrogen and oxygen. The half-cycle termination voltage threshold has been limited. The equilibrium potential values for the cathodic and anodic processes  $e_k$  and  $e_a$  were optimized by limiting the voltage of the reaction on the electrodes (Fig. 7).



(a)



(b)

Figure 7. The cyclogram of the voltage change of the high-pressure hydrogen generator with a voltage limitation from 1.8 V to 0.5 V at  $J = 0.02 \text{ A/cm}^2$  with the electrode twins Ni - Fe (g): (a) - the half-cycle of H<sub>2</sub> generation; (b) - the half-cycle of O<sub>2</sub> generation.

Fig. 7 shows that the voltage limiting of the reaction on the electrodes affects the half-cycle of hydrogen evolution (Fig. 7 a) and, accordingly, the half-cycle of oxygen evolution (Fig. 7 b). At the same time, the amount of H<sub>2</sub> and O<sub>2</sub> released and the dynamics of the releases were measured (Fig. 8).

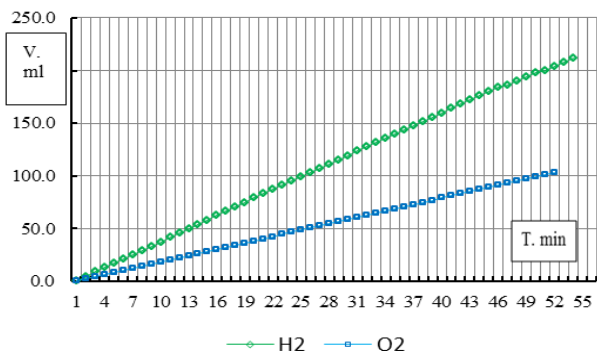


Figure 8. The dynamics of hydrogen and oxygen generation: - limiting the voltage of the reaction from 0.5 to 1.8 V; - current density  $I = 0.02 \text{ A/cm}^2$ ; - electrode twins Ni - Fe(g).

As it is seen from Fig. 8, the dynamics of hydrogen and oxygen evolution is preserved and does not depend on the limitation of the voltage of the reaction at the electrodes. Half-cycles have shortened in time, but the number of half-cycles has increased.

The experimental results have shown that the electrochemical activity of the gas-absorbing electrode material (Fe(g)) is higher in its characteristics than that of platinum-coated electrodes, and exceeds them in the efficiency of the electrolysis process. Thus, the electricity costs for hydrogen and oxygen production are in the range from  $3.95 \text{ kW}\cdot\text{h/m}^3$  to  $4.16 \text{ kW}\cdot\text{h/m}^3$ . It should also be noted that this process is cyclic, consisting of a half-cycle of hydrogen evolution and a half-cycle of oxygen evolution [16]. The energy consumption on the half-cycle of the hydrogen generation is  $0.88 \text{ kW}\cdot\text{h/m}^3$ , and for the oxygen half-cycle is  $3.28 \text{ kW}\cdot\text{h/m}^3$ .

## VI. DISCUSSION OF RESEARCH RESULTS

With the cyclic operation, there is no need to use proton exchange membranes. This makes it possible to significantly increase the operating pressure of the generated gases up to  $P = 20.0 \text{ MPa}$  and higher. Compressor equipment is used to achieve this level of operating pressure in standard electrolysis systems for producing hydrogen. This limits the common use of these systems at present [17]. Such equipment has several disadvantages: special requirements for maintenance, low efficiency (from 16 % to 30 %), high cost [18]. The absence of gas compressors in the technological scheme makes it possible to successfully use the high-pressure electrochemical hydrogen generator as a buffer energy storage in the energy-technological complexes with alternative energy sources.

The advantage of the described membraneless method of hydrogen production lies in the ability to control the reaction rate (by regulating the current), and, consequently, the consumption of electricity for its generation. This is especially important when using renewable types of energy (sun, wind) as primary energy carriers [19], characterized by inconsistent energy supply [20], as well as in joint operation with power units of thermal power plants and nuclear power plants for smoothing loads during the period of peak energy consumption [21].

Based on the obtained experimental data, the fully functional experimental electrolysis installation for the hydrogen and oxygen high-pressure generation EHP - 0.02 - 150 was manufactured (Fig. 9).



(a)



(b)

Figure 9. Experimental electrolysis installation EHP - 0.02 - 150:  
(a) - view from the side of the reactor compartment; (b) - view from the side of power electronics, control and monitoring systems.

The external view of the reactor compartment with executive devices is shown in Fig. 9 a. The main controls are displayed on the control panel. A smart relay "Zelio Logic" from Schneider Electric was used. This is the relay with the ability to program relay logic [22], time delay, pulse counting, processing signals from both discrete and analog sensors. The ability to transmit data via the SR2 USB01 cable for connection to a USB port [23], via Ethernet protocols and using a GSM modem made it possible to eliminate the need for an operator to stay in the EHP area and ensure high reliability and safety of operation [24].

## VII. CONCLUSIONS

The choice of a gas-absorbing electrode made of a structured material, which is a metal with variable valence, and a gas-evolving electrode with a low reversible potential of cathodic and anodic processes, which does not include expensive platinum group metals, gave the following results:

1. The high reactivity of hydrogen and oxygen evolution using galvanic Ni as a passive electrode indicates a decrease in the overvoltage on the corresponding half-cycles. The low overvoltage of the release of H<sub>2</sub> (0.21 V) and O<sub>2</sub> (0.06 V) at the passive electrode makes it possible to obtain these gases directly from the very beginning of the water electrochemical decomposition (Fig. 3).
2. The reactivity of H<sub>2</sub> (O<sub>2</sub>) evolution using the X18H15 – Fe(g) electrode assembly occupies an intermediate position between Ni-Fe (g) and Fe-Fe (g), which makes it possible to reduce the cost of the electrode system.
3. Optimization of operating modes by limiting the threshold values of the voltage of the electrochemical reaction (in the range of 0.5 - 1 V) makes it possible to minimize the specific energy consumption for the process of H<sub>2</sub> (O<sub>2</sub>) release.
4. Specific electricity consumption in hydrogen and oxygen half-cycles was respectively - 0.88 kWh/m<sup>3</sup> per H<sub>2</sub>↑ and - 3.28 kWh/m<sup>3</sup> per O<sub>2</sub>↑. The total specific electricity consumption for the production of these gases does not exceed 4.16 kWh/m<sup>3</sup>.
5. The considered technology for producing hydrogen and oxygen makes it possible to exclude the consumption of electrical energy associated with a voltage drop across the proton exchange membrane IR<sub>m</sub>, due to its absence. This ensures the generation of H<sub>2</sub> (O<sub>2</sub>) under high working pressure up to P = 20.0 MPa.

## VIII. ACKNOWLEDGMENTS

This work was completed with financial supports from Vietnam Academy of Science and Technology under project of Number:QTUA-0101/18e20.

The research was conducted according to projects No. 13-20 "Metal hydride batteries for systems that supply hydrogen to fuel cells". The research was made within the framework of scientific projects of the target program of scientific research of the National Academy of Sciences of Ukraine: "Development of scientific bases of production, storage, and use of hydrogen in autonomous power supply systems".

## IX. REFERENCES

- [1]. D.R. Lide, "CRC Handbook of Chemistry and Physics", 88th ed., CRC Press, 2007. [http://refhub.elsevier.com/S1002-16\)30324-sbref7](http://refhub.elsevier.com/S1002-16)30324-sbref7)
- [2]. Jensen, J. O., Vestbø, A. P., Li, Q., & Bjerrum, N. J.. "The energy efficiency of onboard hydrogen storage." *Journal of Alloys and Compounds*, 2007, 446, pp. 723-728. <http://www.intechopen.com/books/show/title/energy-efficiency>
- [3]. E.W. Lemmon, M.L. Huber, M.O. McLinden, "NIST Stand." *Ref. Database 23 Ref. Fluid Thermodyn. Transp. Prop. REFPROP*, 2013.
- [4]. Nikolic, V. M., Tasic, G. S., Maksic, A. D., Saponjic, D. P., Miulovic, S. M., & Kaninski, M. P. M. "Raising efficiency of hydrogen generation from alkaline water electrolysis—energy saving." *International Journal of Hydrogen Energy*, 2010, vol. 35, no. 22, pp. 12369-12373.
- [5]. Bard, A. J., & Fox, M. A. "Artificial photosynthesis: solar splitting of water to hydrogen and oxygen." *Accounts of Chemical Research*, 1995, vol. 28, no. 3, pp. 141-145.
- [6]. Iordache, I., Bouzek, K., Paidar, M., Stehlik, K., Töpler, J., Stygar, M., & Zgonnik, V. "The hydrogen context and vulnerabilities in the central and Eastern European countries." *International Journal of Hydrogen Energy*, 2019, vol. 44, no. 35, pp. 19036-19054. <https://doi.org/10.1016/j.ijhydene.2018.08.128>.
- [7]. Solovey, V.V., Shevchenko, A.A., Zipunnikov, M.M., Kotenko, A.L., Nguyen Tien Khiem, Bui Dinh Tri, & Tran Thanh "Development of high pressure membraneless alkaline electrolyzer." *International Journal of Hydrogen Energy*. 2021. <https://doi.org/10.1016/j.ijhydene.2021.01.209>
- [8]. Solovey, V. V., Zipunnikov, M. M., Shevchenko, A. A., Vorobjova, I. O., & Kotenko, A. L. "Energy effective membrane-less technology for high pressure hydrogen electro-chemical generation." *French-Ukrainian Journal of Chemistry*, 2018, vol. 6, no. 1, pp. 151–156. <https://doi.org/10.17721/fujcV6I1P151-156>.
- [9]. Shevchenko, A.A., Zipunnikov, M.M., Kotenko, A.L., Vorobjova, I.O., Semykin, V.M. (2019) "Study of the influence of operating conditions on high pressure electrolyzer efficiency." *Journal of Mechanical Engineering*, vol. 22, no. 4, pp. 53-63. <https://doi.org/10.15407/pmach2019.04.053>
- [10]. Shevchenko, A. "Creation of autonomous and network energy-technological complexes with a hydrogen storage of energy." *Vidnovliuvana Energetika*, 2020, vol. 61, no. 2, pp. 18-27. [https://doi.org/10.36296/1819-8058.2020.2\(61\).18-27](https://doi.org/10.36296/1819-8058.2020.2(61).18-27).

- [11]. Yakimenko, L. M. “Elektroodnyye materialy v prikladnoy elektrokhimii [Electrode materials in applied electrochemistry]”. Moscow: Khimiya, 1977, 264 p. (in Russian).
- [12]. Sukhotin, A. M. “Spravochnik po elektrokhimii [Handbook of electrochemistry]”. Leningrad: Khimiya, 1981, 488 p. (in Russian).
- [13]. Spielrain, E. E., Malysenko, S.P., Kuleshov. G.G. “Introduction to hydrogen energy”. M.: Energoatomizdat, 1984, - 264 p. (in Russian).
- [14]. Tomilov, A. P. “Prikladnaya elektrokhiimiya [Applied electrochemistry]”: A textbook. Moscow: Khimiya, 1984, 520 p. (in Russian).
- [15]. Solovey, V., Zipunnikov, M., & Semikin, V. “Method for Calculating the Feed Water Replenishment Parameters under Electrolysis Process in Electrolyzer ” French-Ukrainian Journal of Chemistry, 2020, vol. 8, no. 2, pp. 168-175. <https://doi.org/10.17721/fujcV8I2P168-175>
- [16]. Solovey, V. V., Zipunnikov, N. N., & Shevchenko, A. A. “Issledovaniye effektivnosti elektrodnykh materialov v elektroliznykh sistemakh s razdelnym tsiklom generatsii gazov [Research of the efficiency of electrode materials in electrolysis systems with a separate cycle of gas generation].” Problemy mashinostroyeniya – Journal of Mechanical Engineering, 2015, vol. 18, no. 1, pp. 72–76 [in Russian].
- [17]. Akbar Dadkhah, Dimitar Bozalakov, Jeroen D.M. De Kooning, Lieven Vandeveld. “On the optimal planning of a hydrogen refuelling station participating in the electricity and balancing markets. International Journal of Hydrogen Energy, 2021, vol. 46, no. 2, pp. 1488-1500. <https://doi.org/10.1016/j.ijhydene.2020.10.130>
- [18]. Buttner, W., Rivkin, C., Burgess, R., Hartmann, K., Bloomfield, I., Bubar, M., & Moretto, P. “Hydrogen monitoring requirements in the global technical regulation on hydrogen and fuel cell vehicles.” International journal of hydrogen energy, 2017, vol. 42, no. 11, pp. 7664-7671.
- [19]. Chang, W. J., Lee, K. H., Ha, H., Jin, K., Kim, G., Hwang, S. T., & Hong, J. S. “Design principle and loss engineering for photovoltaic–electrolysis cell system.” ACS Omega, 2017, vol. 2, no. 3, pp. 1009-1018.
- [20] M. Reuß, J. Reul, T. Grube, M. Langemann, S. Calnan, M. Robinius, R. Schlatmann, U. Rau and D. “Solar hydrogen production: a bottom-up analysis of different photovoltaic– electrolysis pathways.” Stollen, Sustainable Energy Fuels, 2019, Advance Article, <https://doi.org/10.1039/C9SE00007K>
- [21]. Shevchenko, A. A., Zipunnikov, M. M., Kotenko, A. L. “Adaptation of the high-pressure electrolyzer in the conditions of joint operation with TPP and NPP power-generating units.” Scientific Bulletin of National Mining University, 2020, vol. 6. pp. 76 – 82. <https://doi.org/10.33271/nvngu/2020-6/076>
- [22]. Smart relay SR3B261BD. Retrieved from: <https://www.se.com/id/en/product/SR3B261BD/modular-smart-relay-zelio-logic---26-i-o---24-v-dc---clockdisplay/>
- [23]. SR2USB01 : USB PC connecting cable - for smart relay Zelio Logic. Retrieved from:
- [24]. Modem interface - GSM - for communication interface SR2COM01. Retrieved from: <https://www.se.com/id/en/product/SR2MOD02/modem-interface---gsm-for-communication-interface-sr2com01/>